A combined computational and experimental study of the adsorption of sulfur containing molecules on molybdenum disulfide nanoparticles

Article *in* Journal of Materials Research · September 2018

DOI: 10.1557/jmr.2018.309

CITATIONS
0

READS
9

11 authors, including:

Hui Ge
Chinese Academy of Sciences
35 PUBLICATIONS **305** CITATIONS
SEE PROFILE

Hao Li
National Institute of Clean-and-Low-Carbon Energy, Beijing
8 PUBLICATIONS **20** CITATIONS
SEE PROFILE

Qing Peng
University of Michigan
105 PUBLICATIONS **1,256** CITATIONS
SEE PROFILE

Manuel Ramos
Universidad Autónoma de Ciudad Juárez
43 PUBLICATIONS **155** CITATIONS
SEE PROFILE

A combined computational and experimental study of the adsorption of sulfur containing molecules on molybdenum disulfide nanoparticles

Tao Yang
State Key Laboratory of Heavy Oil Processing, China University of Petroleum, Beijing 102249, China

Junpeng Feng
State Key Laboratory of Coal Conversion, Institute of Coal Chemistry Chinese Academy of Sciences, Taiyuan, Shanxi 030001, China

Xingchen Liu[a)]
State Key Laboratory of Coal Conversion, Institute of Coal Chemistry Chinese Academy of Sciences, Taiyuan, Shanxi 030001, China; and Synfuels China Co. Ltd., Huairou, Beijing 100195, China

Yandan Wang
State Key Laboratory of Heavy Oil Processing, China University of Petroleum, Beijing 102249, China

Hui Ge and Dongbo Cao
State Key Laboratory of Coal Conversion, Institute of Coal Chemistry Chinese Academy of Sciences, Taiyuan, Shanxi 030001, China

Hao Li
State Key Laboratory of Heavy Oil Processing, China University of Petroleum, Beijing 102249, China

Qing Peng
Nuclear Engineering and Radiological Sciences, University of Michigan, Ann Arbor, Michigan 48109, USA

Manuel Ramos[c)]
Department of Physics and Mathematics, Universidad Autónoma de Cd. Juárez, Juárez 32310, México

Xiao-Dong Wen
State Key Laboratory of Coal Conversion, Institute of Coal Chemistry Chinese Academy of Sciences, Taiyuan, Shanxi 030001, China; and Synfuels China Co. Ltd., Huairou, Beijing 100195, China

Baojian Shen[b)]
State Key Laboratory of Heavy Oil Processing, China University of Petroleum, Beijing 102249, China

(Received 25 June 2018; accepted 10 August 2018)

Combining density functional theory calculations and temperature programmed desorption (TPD) experiments, the adsorption behavior of various sulfur containing compounds, including C_2H_5SH, CH_3SCH_3, tetrahydrothiophene, thiophene, benzothiophene, dibenzothiophene, and their derivatives on the coordinately unsaturated sites of $Mo_{27}S_x$ model nanoparticles, are studied systematically. Sulfur molecules with aromaticity prefer flat adsorption than perpendicular adsorption. The adsorption of nonaromatic molecules is stronger than the perpendicular adsorption of aromatic molecules, but weaker than the flat adsorption of them. With gradual hydrogenation (HYD), the binding affinity in the perpendicular adsorption modes increases, while in flat adsorption modes it increases first, then decreases. Significant steric effects on the adsorption of dimethyldibenzothiophene were revealed in perpendicular adsorption modes. The steric effect, besides weakening adsorption, could also activate the S–C bonds through a compensation effect. Finally, by comparing the theoretical adsorption energies with the TPD results, we suggest that HYD and direct-desulfurization path may happen simultaneously, but on different active sites.

Address all correspondence to these authors.
[a)]e-mail: liuxingchen@sxicc.ac.cn
[b)]e-mail: baojian@cup.edu.cn
[c)]This author was an editor of this journal during the review and decision stage. For the *JMR* policy on review and publication of manuscripts authored by editors, please refer to http://www.mrs.org/editor-manuscripts/.
DOI: 10.1557/jmr.2018.309

I. INTRODUCTION

Hydrodesulfurization (HDS) is an important reaction during the refining process of crude oil for low contaminant liquid fuel production.[1,2] HDS is characterized by the sulfur removal from sulfur-containing molecules as contained in crude oils, reducing sulfur emissions after

combustion. Even though molybdenum disulfide (MoS_2) nanoparticles have been widely used as HDS catalysts for decades, their atomic level HDS mechanism is still not very clear. In recent years, stringent environmental regulations[3] on the sulfur level in fuels have renewed the interest in the understanding of HDS mechanisms, which is essential for developing efficient catalysts and processes for deep HDS.

Sulfur-containing molecules in petroleum or synthetic oils are generally classified into two types: nonheterocycles and heterocycles (Scheme 1). The former includes thiols, sulfides, and disulfides. Heterocycles mainly include thiophene and its derivatives with one or several fused aromatic rings and their alkyl or aryl substituents. In heterocycles, thiophene is a widely used model for the HDS process on MoS_2 in both experiment[4–8] and theory,[9–14] while benzothiophene (BT), dibenzothiophene (DBT), and their derivatives have been widely used as models for deep HDS of fuels in experiment.[15–17] Nonheterocycles, on the other hand, may compete with heterocycles in adsorption and subsequent surface reactions.

Previous efforts to establish the HDS reaction pathways of thiophene[18] and BT[19] applying density functional theory (DFT) methods in MoS_2 revealed that the energy profiles depend on the adsorption mode, which further depend on the sulfur coverage of MoS_2 active sites. Hence, determination of the detailed adsorption mode of the sulfur containing molecules on various sites of MoS_2 is still of vital importance in understanding the HDS mechanism.

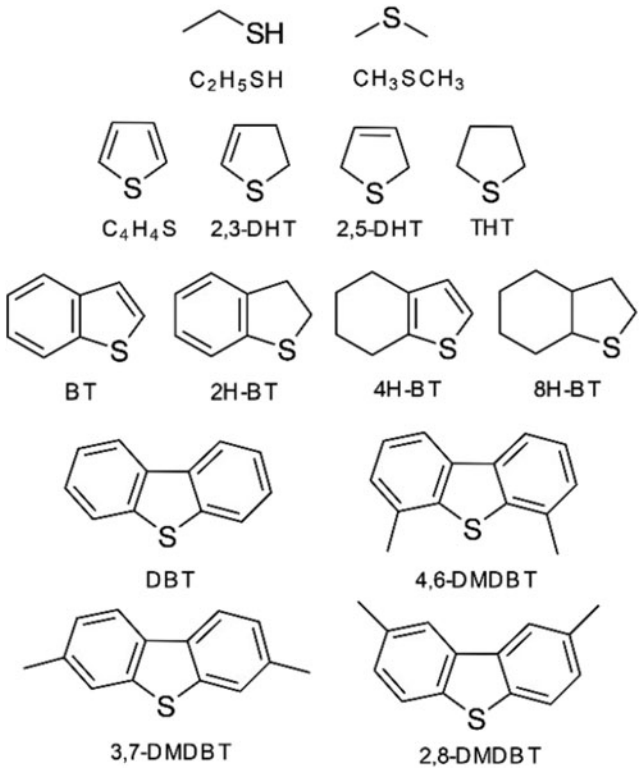

SCHEME 1. Sulfur-containing compounds and their numbering systems.

The adsorption and reaction of thiols (CH_3SH[20] and C_2H_5SH[21]) on the metallic edge of 2H-MoS_2 was studied by Todorova et al. Yogesh et al.[22] calculated the adsorption energies of various sulfur containing molecules on Co/MoS_2 and found the electronic effects on adsorption energies, where it is possible to achieve a linear correlations for prediction of adsorption energies in bimetallic catalyst clusters. A study on similar systems by Šarić et al.[23] shows the preference of physisorption on the S-edges and chemisorption on the Mo-edges.

Thiophene is typically used as a model reactant for understanding the mechanism of HDS. Thiophene adsorption on the crystallographic surfaces[24] and edges[13,14,18,25–27] of MoS_2 has been investigated. The coordinately unsaturated sites (CUS) are found to be the functioning sites, rather than the basal planes, and thiophene could adsorb in both flat and perpendicular modes. Thiophene HDS over MoS_2 catalysts has been studied experimentally by some groups.[28,29] The mechanism proposed by Sullivan et al.[7] suggested that DHT, tetrahydrothiophene (THT), and 1-butanethiolate are intermediates in thiophene HDS.[7,30–35] The HDS of sulfur containing molecules generally proceeds by two pathways: a hydrogenation (HYD) pathway involving aromatic ring HYD, followed by C–S bond cleavage, and a hydrogenolysis pathway via direct C–S bond cleavage without aromatic ring HYD, which is also called the direct desulfurization (DDS) pathway.

Yang et al.[36,37] have studied the adsorption of various methyl-substituted DBT derivatives on a clean Mo edge of $Mo_{10}S_{18}$ cluster by DFT methods and showed the differences among the substituted, nonsubstituted, and hydrogenated derivatives. Using a periodic model, Cristol et al.[38] calculated the adsorption of BT, DBT, and their derivatives on both the S and Mo edges of MoS_2 surfaces. Using similar methods, Moses et al.[24] calculated the adsorption of benzene, thiophene, and BT on the basal plane of MoS_2. Furthermore, the mechanisms of HDS for BT,[39–41] DBT,[15,42,43] and their derivatives have been widely studied.

However, neither a too small cluster nor a too large extended slab are good models of real size MoS_2 nanoparticles, due to the quantum size effect and local structure effects (such as vacancies). First, as the high resolution scanning tunneling microscopy (STM) study[44] reveals, the adsorption properties of MoS_2 nanoclusters toward the HDS refractory DBT vary with cluster size. Second, STM and DFT studies[45] by Tuxen and coworkers suggested the importance of sulfur vacancies in the adsorption of DBT. It has also shown recently that the vacancy plays an important role in determining the thiophene HDS pathway on MoS_2.[46] The breakthrough

in the structural studies of the active nanostructures in HDS using STM[47] motivates us to produce numerical simulations in larger and more realistic MoS_2 nanoparticles.

In this work, we present a study to determine the adsorption of different sulfur-containing molecules including C_2H_5SH, CH_3SCH_3, THT, thiophene, BT, DBT, and their derivatives (Scheme 1) on the CUS of both S and Mo edges of real size $Mo_{27}S_x$ ($Mo_{27}S_{48}$, $Mo_{27}S_{50}$, $Mo_{27}S_{54}$, $Mo_{27}S_{55}$) nanoparticles. Our study is mainly focused on the following three effects: the competition effects of the nonheterocycles with heterocycles; the HYD effects on the adsorption of unsaturated heterocycles and the steric effects of the DBT due to methyl substitution. The calculated adsorption energies are then correlated with the temperature programmed desorption (TPD) experiments, to understand the significance of the adsorption configurations which are found in the theoretical study.

To model the nanometer-sized crystallites observed experimentally, $Mo_{27}S_x$ real size clusters[48] in Fig. 1 are used. The finite slab represents $(\bar{1}010)$ for the S edge and $(10\bar{1}0)$ for the Mo edge of MoS_2. To study the structural and electronic properties of MoS_2, the $Mo_{27}S_{54}$ cluster was used, following the work by Li et al.[49] and Orita et al.[50] Later, in our previous work, the $Mo_{27}S_{54}$ cluster was used to calculate S coverage on both Mo and S edges independently with thermodynamic arguments.[51] There are two types of terminations for MoS_2 edges, Mo-terminated edge (or Mo edge, for short), and S-terminated edge (or S edge). In terms of S coverage, the Mo edge without any additional S atom by definition has 0% S coverage, while the S edge without losing any S atoms by definition has 100% S coverage. The meaning of other sulfur coverages in percentage can be calculated using these two extreme situations as references. In addition, an MoS_2 cluster has two edges, on each end. These two edges are different (one is Mo edge and the other is S edge) to keep the stoichiometry of the cluster close to bulk MoS_2. In this work, based on our previous studies, for sulfur coverage on Mo edges, there are two stable structures with 33 and 50% sulfur coverage on Mo edge; for these two Mo edges, the corresponding S edges on the other side of the cluster have 100% sulfur coverage

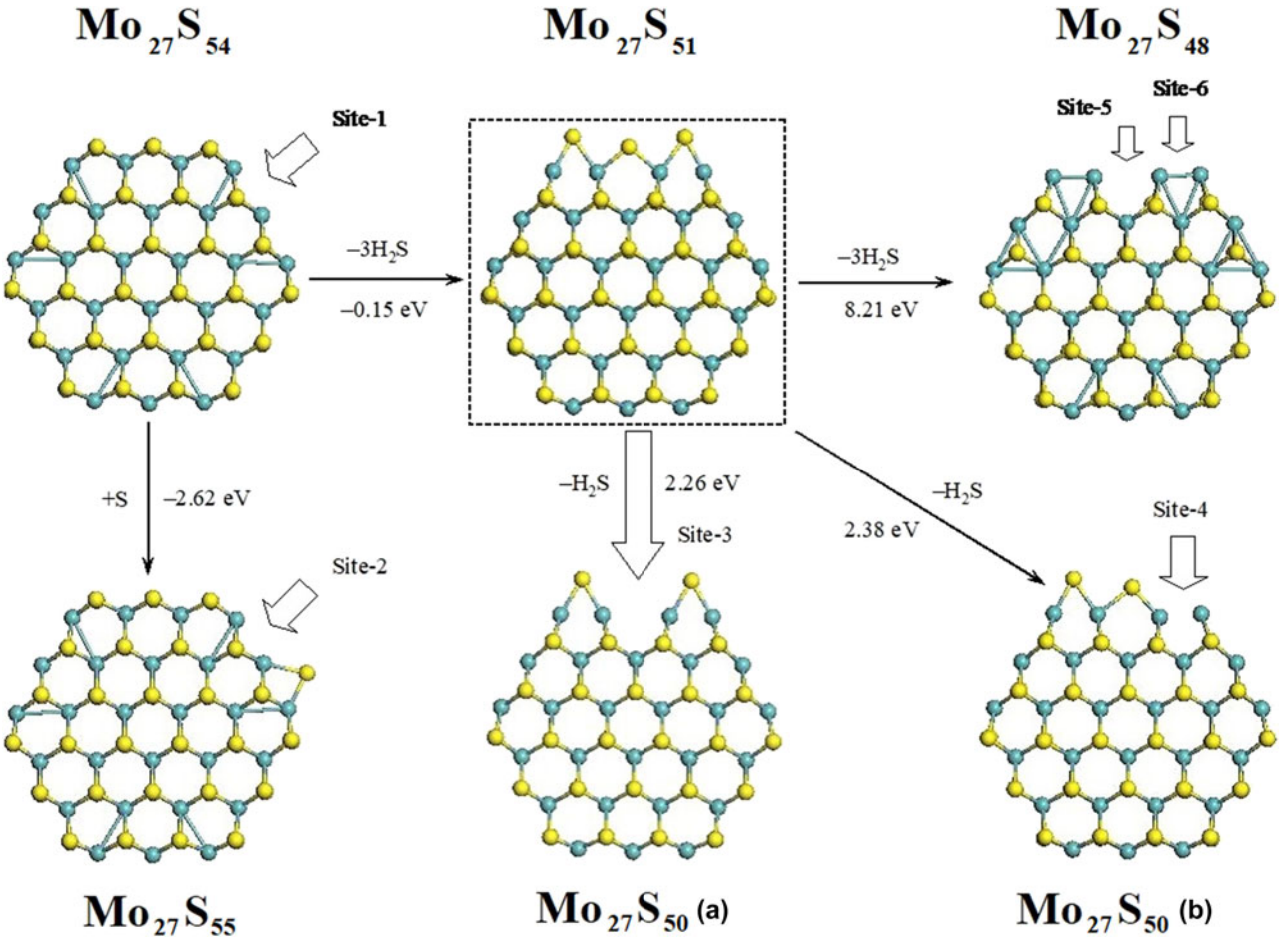

FIG. 1. $Mo_{27}S_x$ (x = 48, 50, 51, 54, 55) clusters. The six adsorption sites and their formation energies are listed. The Mo atoms are in cyan and the S atoms are in yellow.

(33% S on Mo edge & 100% S on S edge, and 50% S on Mo edge & 100% S on S edge). For sulfur coverage on S edge, there is only one stable structure with 67% sulfur coverage on S edge and 0% sulfur coverage on Mo edge (67% S on S edge & 0% S on Mo edge).

To be specific, we have chosen four clusters ($Mo_{27}S_{48}$, $Mo_{27}S_{50}$, $Mo_{27}S_{54}$, $Mo_{27}S_{55}$) for the adsorption of sulfur-containing molecules. The detailed geometric and electronic information about these clusters can be found in our previous studies.[49,51] Six adsorption sites on S edge or Mo edge are chosen in four clusters, as shown in Fig. 1. The studied adsorption sites are named as site-1 to site-6. The adsorption site-1 ($Mo_{27}S_{54}$) and site-2 ($Mo_{27}S_{55}$) are situated on the Mo edge, while site-3 [$Mo_{27}S_{50}$(a)] and site-4 [$Mo_{27}S_{50}$(b)] as well as site-5 ($Mo_{27}S_{48}$) and site-6 ($Mo_{27}S_{48}$) are located on the S edge. There are two adsorption sites (site-3 and site-4) on the S edge with 33% S coverage, and two adsorption sites (site-5 and site-6) on the S edge with 0% sulfur coverage. The sites 3, 4, and 5 are all vacancy sites. As Fig. 1 shows, the formation energies of site-3 and site-4 from the $Mo_{27}S_{51}$ cluster with 50% sulfur coverage on the S edge are 2.26 and 2.38 eV, respectively. The formation energy of site-5 (and site-6) from the $Mo_{27}S_{51}$ cluster with 50% sulfur coverage on the S edge is 8.21 eV. However, the formation energy of site-2 from site-1 by adding one S on the Mo edge is negative (−2.62 eV). These formation energies are calculated from Eq. (1) for adding sulfur on the Mo edge or from Eq. (2) for deleting sulfur on the S edge.

Mo edge:

$$Mo_{27}S_x + nH_2S = Mo_{27}S_{x+n} + nH_2 \quad ,$$

$$\Delta E_{\text{Mo-edge}} = [E(Mo_{27}S_{x+n}) + nE(H_2)] - [E(Mo_{27}S_x) + nE(H_2S)] \quad . \qquad (1)$$

S edge:

$$Mo_{27}S_x + nH_2 = Mo_{27}S_{x-n} + nH_2S \quad ,$$

$$\Delta E_{\text{S-edge}} = [E(Mo_{27}S_{x-n}) + nE(H_2S)] - [E(Mo_{27}S_x) + nE(H_2)] \quad . \qquad (2)$$

Two adsorption modes are considered, one is the μ_2 coordination mode of the sulfur atom bridging two CUS Mo atoms and another is the π-face coordination of the five- or the six-membered aromatic ring. Due to the ring sizes, more continuous CUS Mo atoms are needed for the π-face coordination. Therefore, we use the S edge (0% sulfur coverage, site-5 and site-6) of the $Mo_{27}S_{48}$ cluster and the Mo edge (0% sulfur coverage, site-1) of the $Mo_{27}S_{54}$ cluster.

The adsorption energy for sulfur molecules on these clusters is defined in Eq. (3). The $E_{\text{mol+cluster}}$ is the total energy of the sulfur molecule and the cluster. E_{mol} and E_{cluster} are the total energies of the free sulfur molecule and the cluster, respectively.

$$\Delta E_{\text{ads}} = E_{\text{mol+cluster}} - (E_{\text{mol}} + E_{\text{cluster}}) \quad . \qquad (3)$$

II. METHODS

A. Experimental methods

The MoS_2 powders were first pretreated to 40–60 mesh, then four groups of 100 mg MoS_2 particles were impregnated to sufficient thiophene, thiophane, ethanethiol, and dimethyl sulfide solvent, respectively, for 6 h to guarantee the saturated adsorption. Afterward, the samples were purged with a flow rate of 20 mL/min in argon atmosphere at room temperature overnight. TPD of four organic sulfides over MoS_2 was performed on the instrument of N_2-TPD (TP-5080 version, Xianquan Company, Tianjin, China). Before desorption, 100 mg MoS_2 particles were put into a quartz tube, then it was carried out at a heating rate of 10 °C/min with N_2 (30 mL/min) from room temperature to 110 °C for 1 h to remove the physical adsorption and other impurity on the MoS_2 as much as possible, followed by cooling to 30 °C. Then, the samples were heated to 900 °C at a rate of 10 °C/min with a He flow (30 mL/min), and the tail gas was detected by using a mass spectrometer (Omnistar TM, Asslar, Germany). Following the same operational protocol, the TPD of four organic sulfides chemisorbed on the MoS_2 with a 10 vol% H_2/N_2 mixture (30 mL/min) was performed with the same instruments.

B. Theoretical calculations

All calculations were performed with program package DMol[3] in the Materials Studio package of Accelrys Inc., San Diego, California. The physical wave functions were expanded in terms of accurate numerical basis sets.[52–54] The doubled numerical basis set with p-polarization function (DNP) for hydrogen and d-polarization functions for other elements was used, while the Stuttgart quasi-relativistic effective core potential[55,56] was used for molybdenum, for which the 28 core electrons are treated as effective potential, and the outer 14 valence electrons are treated explicitly. In the numerical basis set of DMol3, the atomic basis sets are generated numerically, and the atomic orbitals are exact spherical. Therefore, the molecule can be dissociated exactly to its constituent atoms, and the basis set superposition error (BSSE) is minimized. As was benchmarked in the literature,[57] the BSSE corrections in dMol3 DNP are less than those in the Gaussian 6-311+G (3*df*,2*pd*) basis set. The generalized gradient corrected functional by Perdew and Wang (GGA-PW91)[58] was used and the numerical integration was performed with medium quality mesh size. The tolerances of energy, gradient, and displacement

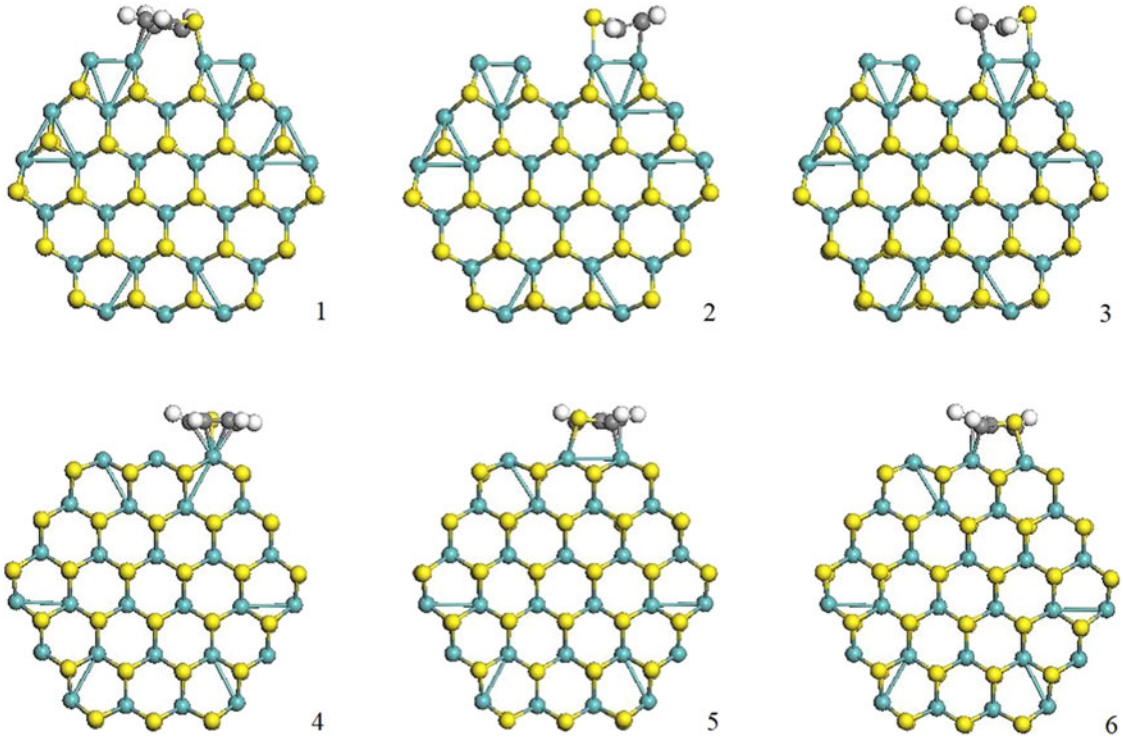

FIG. 2. Different flat adsorption structures for thiophene. Adsorption on S edge (0% sulfur coverage) is shown in structures 1, 2, and 3. Adsorption on Mo edge (0% sulfur coverage) is shown in structures 4, 5, and 6. The Mo atoms are in cyan and the S atoms are in yellow.

convergence are 2×10^{-5} au, 4×10^{-3} au/Å, and 5×10^{-3} Å, respectively. The real space cutoff of atomic orbitals is set at 5.5 Å, and a Fermi smearing of 0.002 is used for orbital occupancy. We compare the smearing 0.002 and 0.0005 by using the structures 1 (shown in Fig. 2) with thiophene flat adsorption on the $Mo_{27}S_{48}$ cluster. The adsorption energy is −2.217 and −2.219 eV, respectively, that is, the adsorption energy difference is very little. These conditions have been used in our previous studies[59] and showed accurate results.

TABLE I. Calculated adsorption energies (ΔE_{ads}, eV) for the different sulfur molecules on different adsorption sites by the perpendicular adsorption mode.

Sites	C_2H_5SH	$CH_3S–CH_3$	THT	Thiophene	BT	DBT
Site-1	−1.65	−1.72	−1.93	−1.03	−1.33	−1.37
Site-2	−1.24	−1.42	−1.56	−0.57	−0.88	−0.98
Site-3	−1.90	−2.11	−2.15	−1.23	−1.42	−1.55
Site-4	−1.32	−1.49	−1.62	−0.67	−0.89	−1.05
Site-5	−1.90	−2.05	−2.13	−1.35	−1.58	−1.72
Site-6	−1.61	−1.72	−1.80	−1.15	−1.37	−1.51

III. RESULTS AND DISCUSSION

A. Adsorption of different sulfur containing molecules

1. μ_2 coordination

Since all the sulfur containing molecules have an S atom, these S atoms can bind to the catalyst clusters through a Mo–S–Mo bridge, which is called μ_2 coordination in coordination chemistry. Geometrically, in μ_2 coordination, all the molecules adsorb on the $Mo_{27}S_x$ clusters in a perpendicular way. The adsorption energies for the different sulfur-containning molecules on different sites in μ_2 coordination are listed in Table I. The calculated negative adsorption energies indicate that all the adsorptions are exothermic. THT as a nonaromatic heterocycle has stronger adsorption than those of C_2H_5SH and CH_3SCH_3 at all the possible adsorption sites. It also shows that CH_3SCH_3 has stronger adsorption than C_2H_5SH. For the aromatic heterocycles, DBT has the strongest adsorption energies compared to BT and thiophene, indicating that the fused benzene rings in BT and its derivatives enhance the adsorption compared to the five-member ring molecule of thiophene. The rank of the magnitude of adsorption energy follows the order of THT > CH_3SCH_3 > C_2H_5SH > DBT > BT > thiophene for all adsorption sites. Clearly, the adsorption of nonaromatic molecules is generally more stronger than the aromatic molecules in the perpendicular adsorption modes.

2. π-Face coordination

In addition to the μ_2 coordination, the aromatic heterocycles including thiophene, BT, and DBT can also bind

TABLE II. Calculated adsorption energies (ΔE_{ads}, eV) for the different sulfur molecules on different adsorption sites by flat adsorption modes. The corresponding structure is labeled as bolded numbers in the parentheses.

	S edge (0% sulfur coverage)			Mo edge (0% sulfur coverage)		
Thiophene	−2.22 (1)	−2.67 (2)	−2.64 (3)	−1.69 (4)	−2.68 (5)	−2.68 (6)
BT	−3.80 (7)		−3.23 (8)		−2.37 (9)	
DBT	−3.09 (10)		−3.50 (11)		−3.33 (12)	

to the $Mo_{27}S_x$ clusters with their aromatic rings through π electrons, which is called π-face coordination (Table II). Because of the parallel nature of the aromatic rings with the cluster surfaces, in all the π-face coordination configurations, the molecules sit flat on the surface and are in the flat adsorption mode. This adsorption mode has been discussed on the S edge (0% sulfur coverage) of $Mo_{27}S_{48}$ cluster on site-5 and site-6, and the Mo edge (0% sulfur coverage) of $Mo_{27}S_{54}$ on site-1. As shown in Fig. 2, structures 1, 2, and 3 are the adsorption geometries with thiophene on S edge (0% sulfur coverage) of $Mo_{27}S_{48}$. Thiophene in structure 1 is adsorbed on two edge Mo atoms, while thiophene in structures 2 and 3 adsorbs on one edge Mo and one corner Mo. Meanwhile, the S atom in thiophene of structures 2 and 3 is bonded with an edge Mo, and a corner Mo atom on the S edge with 0% sulfur coverage, respectively. Structures 2 (−2.67 eV) and 3 (−2.64 eV) are energetically more stable than structure 1 (−2.22 eV) (Table II).

Structures 4, 5, and 6 show the cases of the thiophene adsorption on the Mo edge (0% sulfur coverage) of $Mo_{27}S_{54}$. Structure 4 is thiophene adsorption on one corner Mo atom, while the thiophene in structures 5 and 6 is adsorbed on one corner Mo and one edge Mo atom. In structure 5, the S atom in thiophene is bonded with an edge Mo atom, while in structure 6, the S atom is bonded with a corner Mo atom. The adsorption energies for structures 5 and 6 (−2.68/−2.68 eV) are both higher than 4 (−1.69 eV), indicating that the adsorption of thiophene is more favorable on two CUS Mo atoms.

The structures of BT π-face coordination are shown in Fig. 3. BT is adsorbed on the S edge (0% sulfur coverage) of the $Mo_{27}S_{48}$ cluster in structures 7 and 8. Structure 7 features the BT molecule adsorbed on two edge Mo atoms, with the thiophene ring in BT binding with one of the edge Mo atoms. The BT in structure 8 is adsorbed on one corner Mo and two edge Mo atoms, and the thiophene ring is adsorbed on the two edge Mo atoms. The adsorption structure 8 can be seen as the BT molecule moved overall to right side from its position in structure 7. Structure 9 displays the structure of BT adsorption on the Mo edge (0% sulfur coverage) of the $Mo_{27}S_{54}$ cluster, and the thiophene ring is adsorbed on one corner Mo and one edge Mo atom. However, it is interesting that the benzene ring in structure 9 is slightly tilted off from the thiophene ring, suggesting the possible destabilizing the aromaticity of the molecule by weakening the in-plane π-bonding. To some degree, the interaction between the benzene ring in structure 9 and CUS is decreased; this may affect the adsorption energy of structure 9. As shown in Table II, the adsorption energy of structure 7 is highest in magnitude among the three adsorption structures.

The structures of DBT π-face coordination on the $Mo_{27}S_x$ clusters are also shown in Fig. 3. There are three adsorption structures with DBT having a flat adsorption. In structures 10 and 11, DBT is adsorbed on a $Mo_{27}S_{48}$ cluster. The two benzene rings in DBT of structure 10 are adsorbed on two separate edge Mo atoms, with the thiophene ring being placed between the two edge Mo atoms. By moving DBT in structure 10 right in the plane, we get structure 11, with the thiophene ring in DBT adsorption on one edge Mo atom. In structure 12, DBT is adsorbed on two corner Mo atoms and one edge Mo atom, and the thiophene ring is binding with an edge Mo atom. The adsorption energies for structures 10, 11, and 12 are −3.09, −3.50 and −3.33 eV, respectively, as shown in Table II. Comparing the adsorption energies of structures 10 and 11, it is clear that the adsorption energy of DBT strongly depend on how the thiophene ring in the DBT molecule interacts with the nanoparticles. The adsorption mode with the molecule binding with more coordinated Mo atoms is more preferred than those binding with less coordinated Mo atoms. Specifically in structure 11, the additional coordinated Mo atom binds with the S atom in DBT.

How significant is the competition effect between the adsorption of nonaromatic sulfur-containing molecules and that of the aromatic ones? To answer this question, we would need to compare the adsorption of the two types of molecules in their most stable adsorption geometries, i.e., perpendicular adsorption for nonaromatic ones (Table I) and flat adsorption for aromatic ones (Table II). Clearly, large aromatic molecules such as BT and DBT are much stronger than the nonaromatic ones such as C_2H_5SH and CH_3–S–CH_3 by more than 1 eV, therefore we do not expect much competition effect exist between these two types of molecules. However, small aromatic molecules such as thiophene have, especially at low sulfur coverage sites, comparable adsorption energy with C_2H_5SH and CH_3–S–CH_3. Therefore, much compeition effect is expected to exist between these two types of molecules.

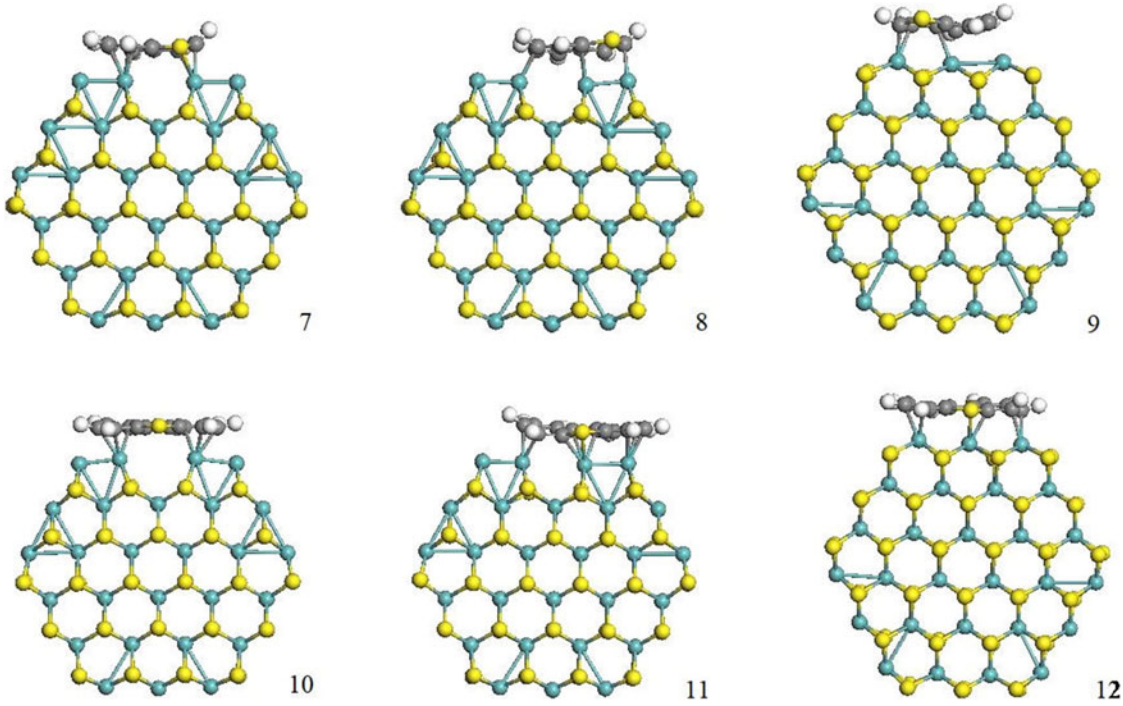

FIG. 3. Different flat adsorption structures for BT (7, 8, 9) and DBT (10, 11, 12). Adsorption on S edge (0% sulfur coverage), as shown in structures 7, 8, 10, and 11. Adsorption on Mo edge (0% sulfur coverage), as shown in structures 9 and 12. The Mo atoms are in cyan and the S atoms are in yellow.

B. Effect of HYD for thiophene and BT

1. μ_2 coordination on site-2, site-3, and site-4

Few groups have reported the comparison of the adsorption of thiophene and BT compounds with their hydrogenated derivatives. For DBT and its hydrogenated derivatives, only Yang et al.[36] discussed the effect of HYD on the Mo edge of the $Mo_{10}S_{18}$ cluster. To understand the effect of HYD for thiophene and BT, we compare these adsorption energies with different sites among thiophene, BT, and their hydrogenated derivatives. The group including thiophene, 2,3-DHT, 2,5-DHT, and THT is discussed to understand the effect of HYD for thiophene, while the group including BT, 2H-BT (HYD in thiophene ring), 4H-BT (HYD in benzene ring), and 8H-BT (HYD in all ring) is used to study the effect of HYD for BT.

It has been indicated by many experiments that the –SH group plays an important role in HYD and HDS.[47,60,61] Particularly, if there are sulfur atoms on this adsorption sites of site-2, site-3, and site-4, then the –SH groups can be formed in these adsorption sites to offer hydrogen atoms for HYD. Therefore, the adsorption structures with perpendicular adsorption for the sulfur molecules are studied on site-2, site-3, and site-4.

All the adsorption energies for the group of thiophene and its hydrogenated derivatives are listed in Table III. The magnitude of the adsorption energies of hydrogenated derivatives on site-2, site-3, and site-4 is higher than that of thiophene on the same sites. Among the three sites, all the molecules in this group prefer site-3 than site-2 or site-4. On the same adsorption sites, the order of adsorption energies in magnitude for these thiophene compounds is THT > 2,5-DHT ≈ 2,3-DHT > thiophene. There are little

TABLE III. Calculated adsorption energies (ΔE_{ads}, eV) for the hydrogenated thiophene, BT, and DBT on different adsorption sites (μ_2 coordination on site-2, site-3, and site-4; and π-face coordination to the Mo edge site).

Sites	Thiophene	2,3-DHT	2,5-DHT	THT
Site-2	−0.57	−1.50	−1.48	−1.56
Site-3	−1.23	−1.95	−2.03	−2.15
Site-4	−0.67	−1.40	−1.45	−1.62
Mo edge	−2.68	−2.80	−2.67	−1.48
Sites	**BT**	**2H-BT**	**4H-BT**	**8H-BT**
Site-2	−0.88	−1.46	−0.93	−1.55
Site-3	−1.42	−2.00	−1.45	−2.13
Site-4	−0.89	−1.45	−0.93	−1.77
Mo edge	−2.37	−2.83	−2.65	−1.55
Sites	**DBT**	**4,6-DMDBT**	**3,7-DMDBT**	**2,8-DMDBT**
Site-2	−0.98	−0.60	−0.96	−1.10
Site-3	−1.55	−1.43	−1.61	−1.61
Site-4	−1.05	−0.93	−1.11	−1.12
Mo edge	−3.33	−3.21	−3.21	−3.52

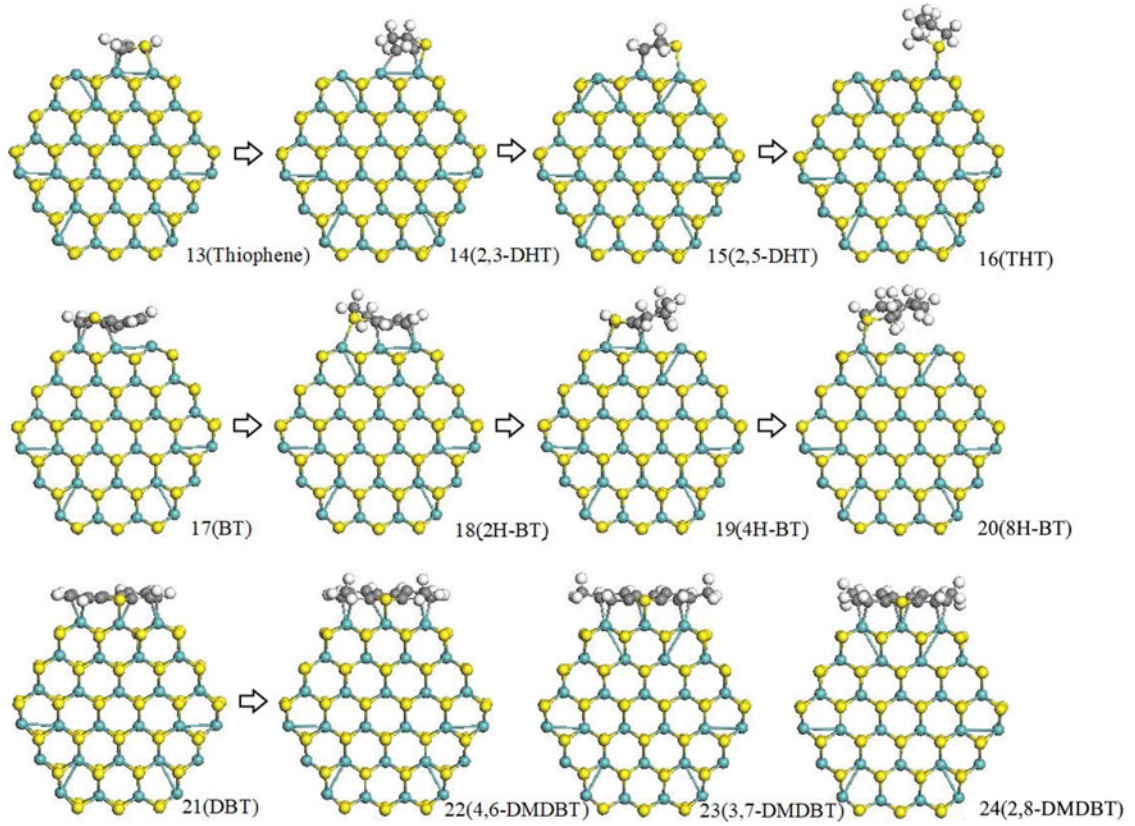

FIG. 4. Different flat adsorption structures for thiophene, BT, DBT and their hydrogenated derivatives. The Mo atoms are in cyan and the S atoms are in yellow.

differences (−0.02/0.08/0.05 eV) of adsorption energies for 2,3-DHT and 2,5-DHT on the same site. From a thermodynamic point of view, they may coexist in the process of HYD or HDS. That is to say, both 2,3-DHT and 2,5DHT are possible intermediates in the reaction of thiophene HDS. From these adsorption energies on different sites, we propose that HYD is more favorable on site-3, in which two S atoms on the tips of the adsorption site, once hydrogenated to –SH, can relocate to more effectively offer hydrogen atoms in the reaction process.

In addition, the adsorption of BT and its hydrogenated derivatives on site-2, site-3, and site-4 are also discussed, with the adsorption energies listed also in Table III. In the three adsorption sites, the adsorption on site-3 is generally more stronger than site-2 and site-4, which is also true for the thiophene compounds as we discussed above. On the same adsorption sites, the adsorption of BT hydrogenated derivatives are stronger than BT itself. The adsorption of 4H-BT with the benzene ring hydrogenated is only slightly stronger than that of BT. However, the adsorption of 2H-BT (with the thiophene ring hydrogenated) and 8H-BT (with complete HYD in all the rings) is much stronger than that of 4H-BT and BT. Our results indicate that 2H-BT and 8H-BT are thermodynamically more strongly binding to the catalyst surfaces and have a higher chance to be observed on the surface. Indeed, the 2H-BT with intermediates in BT HDS have been found on the MoS_2 catalyst in an experiment.[39]

2. π-Face coordination on Mo edge

To compare with perpendicular adsorption, the adsorption of thiophene and BT and their hydrogenated derivatives on the Mo edge by flat adsorption modes are discussed herein as well. The adsorption structures of thiophene and its derivatives are shown in Fig. 4, with the corresponding adsorption energies listed in Table III.

Generally, with HYD, we see an initial rise, then a fall in the magnitude of adsorption energy of both thiophene and BT. The highest point in both cases is the dihydrogenated molecule. However, among 2,3-DHT and 2,5-DHT, the former is thermodynamically more stable than the latter in the flat adsorption model. Once BT is hydrogenated, the hydrogenated part will detach from the adsorption site. The partially hydrogenated BT (2H-BT and 4H-BT) binds to the active site stronger than BT. Comparing the adsorption energies of 2H-BT and 4H-BT, it seems that it is more favorable for HYD to happen at the thiophene ring than at the benzene ring. This is

consistent with the results that are obtained in perpendicular adsorption.

The structures with the weakest adsorption strength are the fully hydrogenated products THT and 8H-BT. Overall, the trend of stronger binding at partial hydrogenated intermediate then much weaker binding at fully hydrogenated product is dramatically different from the trend on the perpendicular adsorption on site-2, 3, and 4 as we discussed earlier. A possible explanation for this is that in flat adsorption modes, the π electrons in the aromatic ring play an important role in the interaction between the molecules and the surfaces.[62] When the aromatic rings are completely hydrogenated, the loss of the π electrons makes the interaction between the molecule and the nanoparticles much weaker. In the perpendicular adsorption mode, the loss of π electron by HYD does not affect much of this type of interaction.

Yang et al.[36] calculated the adsorption of DBT and its hydrogenated derivatives on the Mo edge (0% sulfur coverage) of the $Mo_{10}S_{18}$ cluster. Their results indicate that the adsorption energy in the flat adsorption mode decreased when the aromatic ring was saturated, while the adsorption energies in the perpendicular mode increased with progressive saturation of DBT. Our results for thiophene, BT, and their hydrogenated derivatives agree with that of Yang et al. in the perpendicular adsorption mode. However, in flat adsorption modes, our results show a different trend to that of Yang et al. From the difference, we propose that the HDS mechanism for thiophene and BT may be different from that of DBT, and that the HDS mechanism of the different types of sulfur molecules needs to be studied separately.

C. The steric effect for DMDBT

1. μ_2 coordination on site-2, site-3, and site-4

To understand the steric effect on the adsorption of DMDBT, we investigated the adsorption steric effect at site-2, site-3, and site-4, where steric effects are likely to be significant. The sulfur molecules of 4,6-DMDBT, 3,7-DMDBT, and 2,8-DMDBT are adsorbed on the three sites by the perpendicular adsorption mode. For comparision, the case of DBT adsorption on these three sites is also presented (Table III).

For all three substituted DMDBT isomers, the adsorptions are strongest at site-3. This is in accordance with our previous studies on μ_2 coordination. It is interesting that the adsorption of 4,6-DMDBT is weakest on the same adsorption site, which clearly indicates that the methyl groups in the 4,6-positions prevent the main body of the molecule from approaching the catalyst surface in the perpendicular adsorption model. This type of steric effect in 4,6-DMDBT manifests itself in the all three adsorption sites. By comparing the difference (0.38 eV on site-2; 0.12 eV on site-3; 0.12 eV on site-4) in adsorption energy between DBT and 4,6-DMDBT on the same site, it is clear that the difference (0.38 eV) is mostly on site-2. Meanwhile, the adsorption energy of 3,7-DMDBT (−0.96 eV) on site-2 is lower in magnitude than that of 2,8-DMDBT (−1.10 eV), while the adsorption energy for 3,7-DMDBT on site-3 and site-4 is similar compared with that of 2,8-DMDBT. These results show that site-2 (Mo egde with S atom) is very sensitive to the steric effect. In fact, not only 4,6-DMDBT but also 3,7-DMDBT have clear steric effects on site-2.

To evaluate the activation of the S–C bonds in these DMDBTs, the S–C bond lengths in the adsorbed molecules are shown in Table S1. Although the adsorption energy of 4,6-DMDBT is the weakest, the S–C bond lengths in 4,6-DMDBT (1.812 Å on average) on the three adsorption sites are consistently longer than the other DMDBT molecules (1.793 Å on average). The reason for the greater activation of the S–C bond in 4,6-DMDBT is probably because of the stronger steric effect caused by the two methyl groups in 4,6-positions. These two down-pointing methyl groups prevent the binding interactions between the two sides of the molecule with the nanoparticles, leaving only the central S atom as the effective interaction channel. As such, more electrons can be transferred from the central S atom in DMDBT to the nanoparticle. Thus the S–C bonds are weakened more than other isomers of DMDBT, and we see a more stretched S–C bond length in 4,6-DMDBT. Our results suggest that the steric effect does not only weaken the overall binding of the molecule with the nanoparticle as everyone realize but also can slightly enhance the activation of the key chemical bonds (like S–C) through a compensation effect.

2. π-Face coordination on the Mo edge

The optimized structures of DBT and DMDBTs on the Mo edge with flat adsorption modes are shown in Fig. 4, and the adsorption energies are listed in Table III. The adsorption energies are the same for 4,6-DMDBT and 3,7-DMDBT. Also, the adsorption energy for DBT and 2,8-DMDBT is only slightly higher than that of 4,6-DMDBT and 3,7-DMDBT. The obtained structures show that in flat adsorption modes, all the methyl groups in the DMDBT derivatives are streched out of the plane and have little steric interaction with the nanoparticle.

To evaluate the degree of the steric effect quantitatively, we define an adsorption energy error (n%) using 4,6-DMDBT as an example. That is, $n\% = [E_{ads(4,6\text{-DMDBT})} - E_{ads(DBT)}]/E_{ads(DBT)}$. From our calculation, $n\%$ varies from −7.7 to −38.8% when these sulfur molecules are adsorbed in perpendicular adsorption modes. However, in flat adsorption modes, $n\%$ is only −3.6%. This indicates that the steric effect from flat adsorption is much smaller than that from perpendicular

adsorption. However, due to the loss of steric effect, as we argued ealier, the S–C bonds will be less weakened. Indeed, as Table S-1 shows, the S–C bond lengths of all the molecules in flat adsorption modes on the Mo-edges are consistently shorter than that on those sites with steric effects (site-2, site-3, and site-4).

There are some experimental studies on the rate of the HDS for DBT and DMDBTs.[43,63–66] The rate of DBT conversion is slightly higher than that of 3,7-DMDBT and 2,8-DMDBT and is about 10 times higher than that of 4,6-DMDBT. Under conventional HDS conditions, the DDS pathway contributed 80% to the overall HDS of DBT, while only 20% to the HDS of 4,6-DMDBT. It was shown that the presence of methyl groups in the 4 and 6 positions in 4,6-DMDBT inhibited the DDS pathway, whereas the HYD pathway was hardly affected. Meanwhile, the low reactivity of 4,6-DMDBT is mainly due to the inhibition of the DDS pathway.[2] Since the adsorption energies for 4,6-DMDBT on the three adsorption sites are lower than that for DBT, the steric effects are most significant if the methyl groups are located in the 4 and 6 positions of DMDBT.

There is still a controversy on active sites for HYD (HYD reactions) and DDS (hydrogenolysis of the C–S bonds). Some authors[64] propose that a single site is the origin of both reactions. Others[63] suggest that there are two different active sites by the inhibiting effect of H_2S that H_2S inhibits the DDS more strongly than the HYD path. The DFT calculation results of Cristol et al.[14,38] support the latter. Our results imply that the HYD and DDS processes begin from the flat adsorption and perpendicular adsorption models, respectively, therefore supporting the latter argument.

First, DBT favors the adsorption on site-1 (Mo edge) with flat adsorption, while it favors adsorption on site-3 with perpendicular adsorption. If we accept the hypothesis that site-1 (Mo edge) and site-3 are possible HYD and DDS active sites, then the fact of H_2S inhibition effect can be explained. We have calculated the adsorption of H_2S on site-1, site-2, site-3, and site-4. The adsorption energy is −1.06 eV, −0.77 eV, −1.44 eV, and −1.29 eV, respectively. In other words, it is easier for H_2S to deposit a sulfur atom on site-3 than site-1 and site-2. This shows that the active sites of DDS are more strongly affected than those of HYD by the deposition of sulfur from H_2S. Accordingly, the number of site-3 (DDS active sites) will be decreased under the presence of H_2S; thus, the rate of DDS path may be affected more than the HYD path. Indeed, the preference of HYD over DDS is confirmed by the experiment.[67]

Another possible hypothesis for site-3 is that it contributed not only to the DDS pathway but also to the HYD pathway. Under HDS conditions, the –SH groups can be easily formed by the binding of the two tip S atoms at site-3 with H atoms from dissociated molecular hydrogen. Then, the atomic hydrogen in the formed –SH groups can migrate from the S atoms to DBT. Therefore, the processes of DDS and HYD can both take place on the site-3, and there would be a ratio that desulfurization happens by the two pathways. This argument is supported by recent experimental studies,[67,68] which shows that the HDS of DBT can happen through both the DDS pathway, yielding biphenyl, and the HYD pathway, yielding cyclohexylbenzene and tetrahydrodibenzothiophene (THDBT, or 4H-DBT in our notation). Due to the different chemical surroundings for the sites, the ratio of DDS/HYD is also different. It is therefore possible to change the ratio of DDS/HYD (in other words, control the reaction selectivity) by changing the ratio of active sites with H_2S. Further validation requires a detailed mechanism study of DBT HDS on different active sites from experimental or theoretical studies.

The difference in the ratio (DDS/HYD) for DBT and 4,6-DMDBT[68] can be understood from our DFT calculations. Since the steric effect in flat adsorption is much smaller than that in perpendicular adsorption, 4,6-DMDBT favors flat adsorption mostly due to steric effects. It is known that HYD would happen more easily if the aromatic molecules are adsorbed in the flat mode, causing a significant destabilizing of the aromatic ring. Therefore, the experimental finding that HYD contributes more to the overall HDS of 4,6-DMDBT can be explained by our theoretical study.

D. Temperature programmed desorption-mass spectroscopy

With the adsorption configurations of sulfur containing molecules on MoS_2 nanoparticles obtained in the above theoretical results, it would be interesting to know which of these configurations contribute more on the actual MoS_2 catalysts than others. For this purpose, we use four model molecules (thiophene, THT, C_2H_5SH, and CH_3SCH_3) to examine the experimental desorption peaks on MoS_2, assuming that the five $Mo_{27}S_x$ nanoparticle models have captured the most important adsorption sites in MoS_2 particles in the experiment.

Figure 5(a) shows the temperature programmed desorption-mass spectra (TPD-MS) of thiophene on MoS_2 with He protection. There are two high desorption peaks, one located at 99 °C and the other narrower one at 408 °C. Besides, a low and broad desorption peak occurs around 200 °C. These observations are generally in agreement with our DFT predictions. Most of the perpendicular adsorption modes have fairly small adsorption strengths, and the range has peaks at 99 and 200 °C. The flat adsorption modes, however, involve quite strong interactions with a very narrow range (−2.22 to −2.68 eV, Table II). The only exception in the flat adsorption

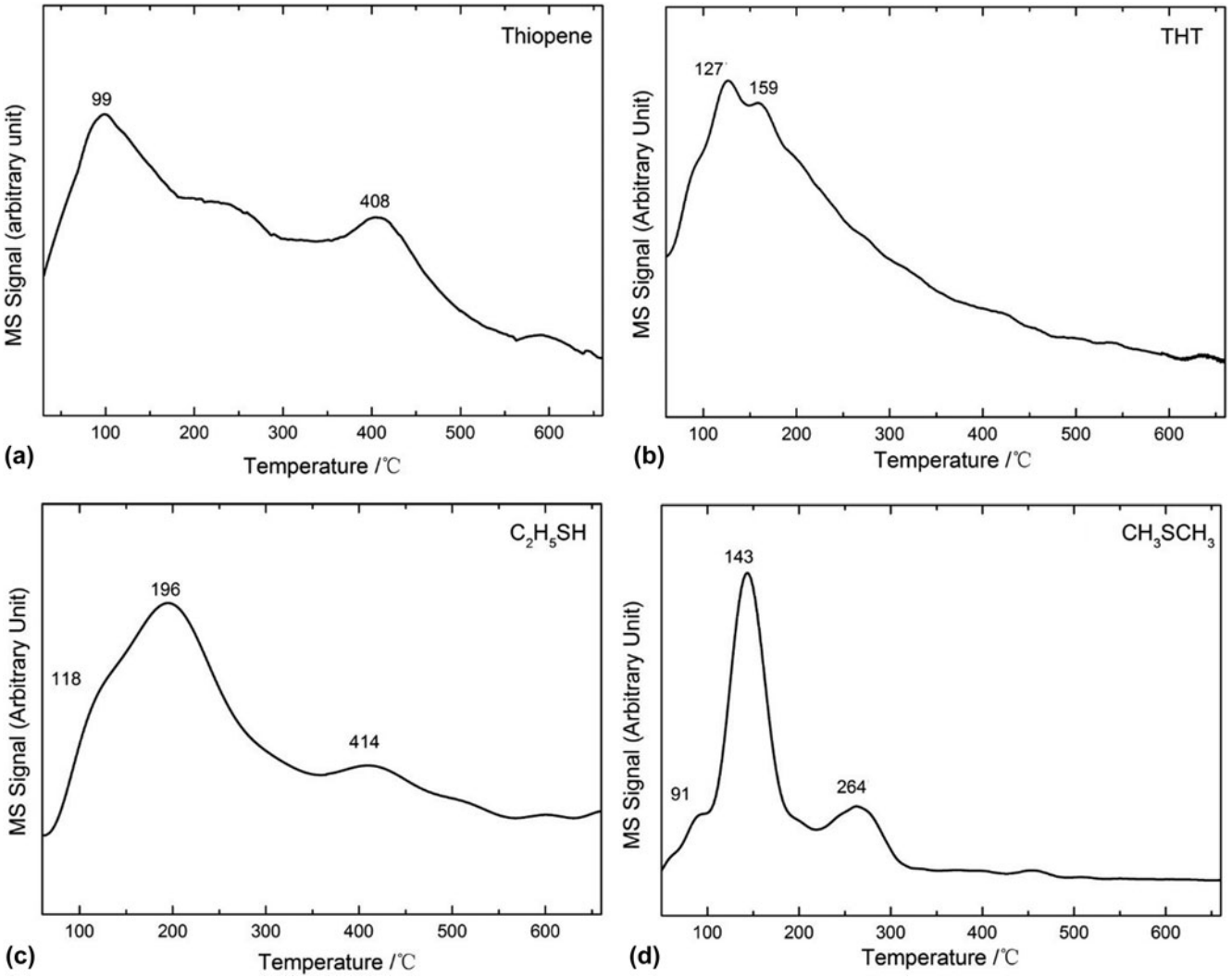

FIG. 5. TPD-MS spectra of thiophene, THT, C_2H_5SH, and CH_3SCH_3 in He protection.

mode with a smaller adsorption energy is the case when thiophene is on the top site of the Mo edge with 0% S coverage (4 in Fig. 2). We can also learn from Fig. 5 that the majority of the thiophene molecules adsorb on the weak-binding sites of Mo_2S such as site-2 and site-4.

In the HYD environment [Fig. 6(a)], thiophene was found to be easily hydrogenated throughout the heating process, yielding sulfur-containing products like C_4H_8S (THT) and $C_4H_{10}S$, and sulfur-free products like C_4H_6 and C_4H_8 through hydrogenolysis and H_2S elimination. This implies that thiophene desulfurization can happen through either DDS or HYD desulfurization, although Moses et al. have suggested that DDS is more favorable.[69] Figure 6(a) also shows that the highest desorption peak of thiophene occurs at about 99 °C, although with partial HYD which forms C_4H_{10} (butane).

Since BT, DBT, and their derivatives are solid in normal conditions, it is extremely difficult to carry out similar TPD studies. However, we can make some reasonable inferences from the case of thiophene. When the aromatic ring extends, the flat adsorption mode would gain more binding strength with the surface, while the perpendicular adsorption mode would not, leading to even larger difference in the adsorption energy and therefore corresponding desorption peaks in TPD. The former inference is in line with our DFT studies. For instance, in Table I, the perpendicular adsorption mode of BT and DBT has adsorption energies of (−0.88 eV to −1.58 eV) and (−0.98 eV to −1.72 eV), respectively. However, as Table II shows, their flat adsorption modes have adsorption energies as large as −3.80 eV and −3.50 eV, respectively.

THT in He protected TPD-MS spectra [Fig. 5(b)] shows two peaks very close to each other at 127 and 159 °C. This suggests that the difference in adsorption configurations does not have much effect on the adsorption energy. Indeed, this matches with our DFT prediction which shows that the adsorption strength is mild,

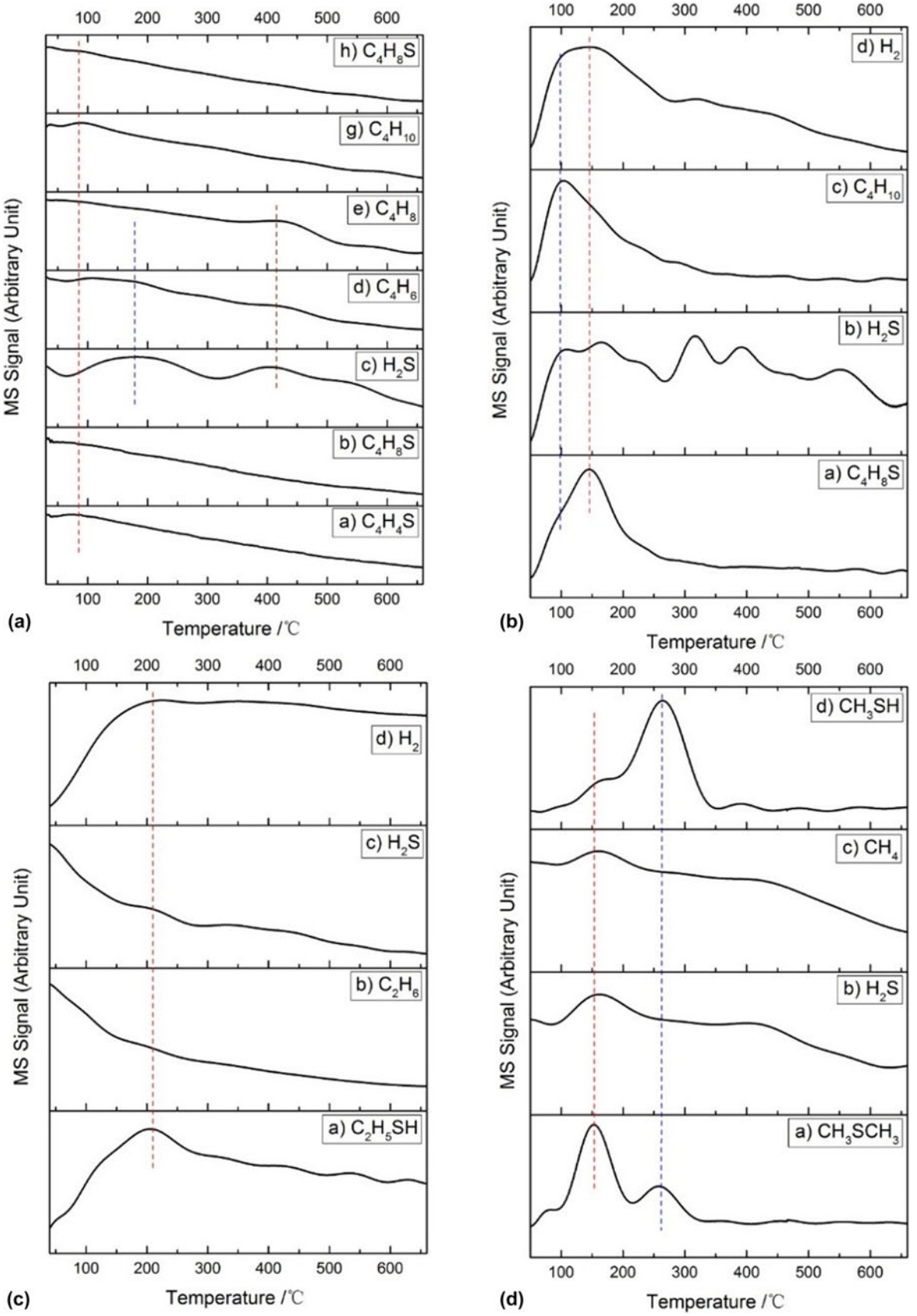

FIG. 6. TPD-MS spectra of thiophene (a), THT (b), C_2H_5SH (c), and CH_3SCH_3 (d) in the mixture of Ar/H_2.

and the range of adsorption energy is relatively narrow, from −1.48 to −2.15 eV (Tables II and III). In the H_2 environment [Fig. 6(b)], THT desulfurization is clearly through HYD, rather than DDS, which is reflected by the simultaneous decrease of the THT signal with H_2 and C_4H_{10} signal from 150 to 300 °C. The major HYD products are butane and H_2S. However, there might be some intermediates that can be directly desulfurized, as the H_2S peaks at 300, 400, and 550 manifest.

The aliphatic sulfur compound C_2H_5SH has a quite unique shape in the TPD profile [Fig. 5(c)]. Instead of a sharp peak, it shows a broad, ascending desorption band between 118 and 196 °C, corresponding to the DFT adsorption energy of −1.24 to −1.90 eV. However, C_2H_5SH has a broad desorption at very high temperature near 400 °C, outside the prediction of DFT. This can be explained by the dissociative adsorption which forms a strongly binding thiolate metal complex C_2H_5S–Mo on the surface.[21] In the HYD environment [Fig. 6(c)], these strongly binding species were hydrogenated, forming C_2H_6 and H_2S. This is evidenced by the disappearance of the high temperature peak at 414 °C in the TPD spectra under N_2/H_2 flowing conditions. This is in accordance with the DFT study,[21] which showed that the C_2H_6 formation has a lower energy barrier than C_2H_4 formation. At low temperature, there are strong H_2S and C_2H_6 signals, accompanied by a weak H_2 signal (suggesting high H_2 consumption), showing that at low temperature, C_2H_5SH desulfurization happens mainly through the HYD mechanism. However, when the temperature is increased, there is still a large amount of C_2H_5SH on the surface, but the existence of high H_2 concentration seems to prohibit the desulfurization process, suggesting that the DDS pathway, although less efficient than HYD, is the only feasible pathway at high temperatures. We can thus propose that the C_2H_5SH desulfurization mechanism is temperature dependent.

As the isomer of C_2H_5SH, CH_3SCH_3 has three peaks on the TPD-MS profile: a sharp one at 143 °C, a shoulder peak at 91 °C, and a broader one at 265 °C [Fig. 5(d)]. The intense sharp peak and its shoulder peak correspond to the weak adsorption sites of site-2, site-4, site-1, and site-6, with adsorption energies between −1.42 and −1.72 eV. The latter broad peak corresponds to the stronger adsorption sites of site-3 and site-5, with adsorption energies of −2.11 eV and −2.05 eV, respectively. In the HYD condition, CH_3SCH_3 has only two HYD products: CH_4 and CH_3SH, showing that the breaking of C–S bond as the only mechanism for its HYD [Fig. 6(d)].

IV. CONCLUSIONS

The adsorption of different sulfur compounds including C_2H_5SH, CH_3SCH_3, THT, thiophene, BT, DBT, and their derivatives have been computed systematically at the level of DFT. More importantly, these sulfur compounds were adsorbed on several different active sites of S and Mo edges for experimental accurate cluster size of the MoS_2 catalyst ($Mo_{27}S_{48}$, $Mo_{27}S_{50}$, $Mo_{27}S_{54}$, and $Mo_{27}S_{55}$) clusters. On the basis of the adsorption energies for sulfur compounds, the order of exothermic energies is THT > CH_3SCH_3 > C_2H_5SH > DBT > BT > thiophene for adsorption on the same adsorption site by perpendicular adsorption modes. Competition of adsorption may exist in these molecules. The adsorption site-2 and site-5 may play a key role on adsorption and activation. The flat adsorption modes are more favorable than the perpendicular adsorption modes for aromatic molecules.

The hydrogenated derivatives of thiophene and BT have been reported in this work to study the effect of HYD on the adsorption energies. It is demonstrated that the adsorption energy in the perpendicular adsorption mode increased when the aromatic ring was saturated. However, under the flat adsorption mode, the adsorption energy for partial hydrogenated thiophene and BT are higher than that of thorough hydrogenated derivatives.

By comparing the adsorption of DBT and two methyl-substituted DBT (DMDBT) adsorption on different sites, the steric effect of 4,6-DMDBT is observed on the adsorption sites studied. Its effect depends on the nature of the adsorption site. Specifically, the steric effect by flat adsorption is smaller than that of by perpendicular adsorption.

The DFT predicted adsorption energies are compared with the He-protected and unprotected TPD experiments. From the comparison, the significance of the theoretical adsorption configurations on experimental MoS_2 particles for the various classes of sulfur-containing molecules can be understood. Our results also support the mechanism that HYD and DDS paths happen simultaneously, but on different active sites.

ACKNOWLEDGMENTS

The authors are grateful for financial support from the National Natural Science Foundation of China (Nos. 21473229, 91545121, 21776304, 21603252, and 21473231), No. 201601D021048 from the Shanxi Province Science Foundation for Youth, and from Synfuels China, Co. Ltd. We also acknowledge the innovation foundation of Institute of Coal Chemistry, Chinese Academy of Sciences, National Thousand Young Talents Program of China, Hundred-Talent Program of Chinese Academy of Sciences, and Shanxi Hundred-Talent Program.

REFERENCES

1. B. Delmon and G.F. Froment: Remote control of catalytic sites by spillover species: A chemical reaction engineering approach. *Cat. Rev.* **38**, 69 (1996).

2. H. Topsøe, B. Clausen, and F. Massoth: Hydrotreating catalysis. In *Catalysis*, J. Anderson and M. Boudart, eds. (Springer Berlin Heidelberg, New York, USA, 1996); p. 1.
3. European Parliament and of the Council, European Directive 98/70/CE of the European Parliament and of the Council, *Official Journal of the European Communities*, **350**, 58 (1998).
4. P. Mills, S. Korlann, M.E. Bussell, M.A. Reynolds, M.V. Ovchinnikov, R.J. Angelici, C. Stinner, T. Weber, and R. Prins: Vibrational study of organometallic complexes with thiophene ligands: Models for adsorbed thiophene on hydrodesulfurization catalysts. *J. Phys. Chem. A* **105**, 4418 (2001).
5. P.C.H. Mitchell, D.A. Green, E. Payen, J. Tomkinson, and S.F. Parker: Interaction of thiophene with a molybdenum disulfide catalyst-an inelastic neutron scattering study. *Phys. Chem. Chem. Phys.* **1**, 3357 (1999).
6. S. Harris and R.R. Chianelli: Catalysis by transition metal sulfides: A theoretical and experimental study of the relation between the synergic systems and the binary transition metal sulfides. *J. Catal.* **98**, 17 (1986).
7. D.L. Sullivan and J.G. Ekerdt: Mechanisms of thiophene hydrodesulfurization on model molybdenum catalysts. *J. Catal.* **178**, 226 (1998).
8. M. Komarneni, A. Sand, and U. Burghaus: Adsorption of thiophene on inorganic MoS_2 fullerene-like nanoparticles. *Catal. Lett.* **129**, 66 (2009).
9. G.D. Atter, D.M. Chapman, R.E. Hester, D.A. Green, P.C.H. Mitchell, and J. Tomkinson: Refined ab initio inelastic neutron scattering spectrum of thiophene. *J. Chem. Soc., Faraday Trans.* **93**, 2977 (1997).
10. J.A. Rodriguez: Interaction of hydrogen and thiophene with Ni/MoS_2 and Zn/MoS_2 surfaces: A molecular orbital study. *J. Phys. Chem. B* **101**, 7524 (1997).
11. H. Toulhoat, P. Raybaud, S. Kasztelan, G. Kresse, and J. Hafner: Transition metals to sulfur binding energies relationship to catalytic activities in HDS: Back to sabatier with first principle calculations1. *Catal. Today* **50**, 629 (1999).
12. X. Ma and H.H. Schobert: Molecular simulation on hydrodesulfurization of thiophenic compounds over MoS_2 using ZINDO. *J. Mol. Catal. A: Chem.* **160**, 409 (2000).
13. P. Raybaud, J. Hafner, G. Kresse, and H. Toulhoat: Adsorption of thiophene on the catalytically active surface of MoS_2: An ab initio local-density-functional study. *Phys. Rev. Lett.* **80**, 1481 (1998).
14. S. Cristol, J-F. Paul, C. Schovsbo, E. Veilly, and E. Payen: DFT study of thiophene adsorption on molybdenum sulfide. *J. Catal.* **239**, 145 (2006).
15. J. Mijoin, G. Pérot, F. Bataille, J.L. Lemberton, M. Breysse, and S. Kasztelan: Mechanistic considerations on the involvement of dihydrointermediates in the hydrodesulfurization of dibenzothiophene-type compounds over molybdenum sulfide catalysts. *Catal. Lett.* **71**, 139 (2001).
16. V. Vanrysselberghe, R. Le Gall, and G.F. Froment: Hydrodesulfurization of 4-methyldibenzothiophene and 4,6-dimethyldibenzothiophene on a CoMo/Al_2O_3 catalyst: Reaction network and kinetics. *Ind. Eng. Chem. Res.* **37**, 1235 (1998).
17. D. Duayne Whitehurst, T. Isoda, and I. Mochida: Present state of the art and future challenges in the hydrodesulfurization of polyaromatic sulfur compounds. In *Advances in Catalysis*, D.D. Eley, W.O. Haag, B. Gates, and H. Knözinger, eds. (Academic Press, 1998); p. 345.
18. P. Raybaud, J. Hafner, G. Kresse, and H. Toulhoat: Ab initio energy profiles for thiophene HDS on the MoS_2 (1010) edge-surface. In *Studies in Surface Science and Catalysis*, G.F.F.B. Delmon and P. Grange, eds. (Elsevier, Amsterdam, the Netherlands, 1999); p. 309.
19. S. Cristol, J.F. Paul, E. Payen, D. Bougeard, J. Hafner, and F. Hutschka: Theoretical study of benzothiophene hydrodesulfurization on MoS_2. In *Studies in Surface Science and Catalysis*, G.F.F.B. Delmon and P. Grange, eds. (Elsevier, Amsterdam, the Netherlands, 1999); p. 327.
20. T. Todorova, R. Prins, and T. Weber: A density functional theory study of the hydrogenolysis reaction of CH_3SH to CH_4 on the catalytically active (100) edge of 2H-MoS_2. *J. Catal.* **236**, 190 (2005).
21. T. Todorova, R. Prins, and T. Weber: A density functional theory study of the hydrogenolysis and elimination reactions of C_2H_5SH on the catalytically active (100) edge of 2H-MoS_2. *J. Catal.* **246**, 109 (2007).
22. Y.V. Joshi, P. Ghosh, P.S. Venkataraman, W.N. Delgass, and K.T. Thomson: Electronic descriptors for the adsorption energies of sulfur-containing molecules on Co/MoS_2, using DFT calculations. *J. Phys. Chem. C* **113**, 9698 (2009).
23. M. Šarić, J. Rossmeisl, and P.G. Moses: Modeling the adsorption of sulfur containing molecules and their hydrodesulfurization intermediates on the Co-promoted MoS_2 catalyst by DFT. *J. Catal.* **358**, 131 (2018).
24. P.G. Moses, J.J. Mortensen, B.I. Lundqvist, and J.K. Nørskov: Density functional study of the adsorption and van der Waals binding of aromatic and conjugated compounds on the basal plane of MoS_2. *J. Chem. Phys.* **130**, 104709 (2009).
25. H. Orita, K. Uchida, and N. Itoh: Adsorption of thiophene on an MoS_2 cluster model catalyst: Ab initio density functional study. *J. Mol. Catal. A: Chem.* **193**, 197 (2003).
26. H. Orita, K. Uchida, and N. Itoh: A volcano-type relationship between the adsorption energy of thiophene on promoted MoS_2 cluster-model catalysts and the experimental HDS activity: Ab initio density functional study. *Appl. Catal., A* **258**, 115 (2004).
27. X-Q. Yao, Y-W. Li, and H. Jiao: Mechanism of thiophene hydrodesulfurization on a Mo_3S_9 model catalyst. A computational study. *J. Mol. Struct.: THEOCHEM* **726**, 81 (2005).
28. K.F. McCarty and G.L. Schrader: Deuterodesulfurization of thiophene: An investigation of the reaction mechanism. *J. Catal.* **103**, 261 (1987).
29. O.G. Salnikov, D.B. Burueva, D.A. Barskiy, G.A. Bukhtiyarova, K.V. Kovtunov, and I.V. Koptyug: A mechanistic study of thiophene hydrodesulfurization by the parahydrogen-induced polarization technique. *ChemCatChem* **7**, 3508 (2015).
30. E.J.M. Hensen, M.J. Vissenberg, V.H.J. de Beer, J.A.R. van Veen, and R.A. van Santen: Kinetics and mechanism of thiophene hydrodesulfurization over carbon-supported transition metal sulfides. *J. Catal.* **163**, 429 (1996).
31. J.T. Roberts and C.M. Friend: Model hydrodesulfurization reactions: Saturated tetrahydrothiophene and 1-butanethiol on molybdenum(110). *J. Am. Chem. Soc.* **108**, 7204 (1986).
32. A.C. Liu and C.M. Friend: Evidence for facile and selective desulfurization: The reactions of 2,5-dihydrothiophene on molybdenum(110). *J. Am. Chem. Soc.* **113**, 820 (1991).
33. E.J. Markel, G.L. Schrader, N.N. Sauer, and R.J. Angelici: Thiophene, 2,3- and 2,5-dihydrothiophene, and tetrahydrothiophene hydrodesulfurization on Mo and Reγ-Al_2O_3 catalysts. *J. Catal.* **116**, 11 (1989).
34. A.E. Hargreaves and J.R.H. Ross: An investigation of the mechanism of the hydrodesulfurization of thiophene over sulfided Co–MoAl_2O_3 catalysts. *J. Catal.* **56**, 363 (1979).
35. J. Devanneaux and J. Maurin: Hydrogenolysis and hydrogenation of thiophenic compounds on a Co–MoAl_2O_3 catalyst. *J. Catal.* **69**, 202 (1981).
36. H. Yang, C. Fairbridge, and Z. Ring: Adsorption of dibenzothiophene derivatives over a MoS_2 nanocluster: A density functional theory study of structure–reactivity relations. *Energy Fuels* **17**, 387 (2003).
37. H. Yang, C. Fairbridge, J. Chen, and Z. Ring: Structure-HDS reactivity relationship of dibenzothiophenes based on density functional theory. *Catal. Lett.* **97**, 217 (2004).
38. S. Cristol, J-F. Paul, E. Payen, D. Bougeard, F. Hutschka, and S. Clémendot: DBT derivatives adsorption over molybdenum sulfide catalysts: A theoretical study. *J. Catal.* **224**, 138 (2004).

39. V.H.J. de Beer, J.G.J. Dahlmans, and J.G.M. Smeets: Hydrodesulfurization and hydrogenation properties of promoted MoS_2 and WS_2 catalysts under medium pressure conditions. *J. Catal.* **42**, 467 (1976).
40. P. Geneste, P. Amblard, M. Bonnet, and P. Graffin: Hydrodesulfurization of oxidized sulfur compounds in benzothiophene, methylbenzothiophene, and dibenzothiophene series over CoO–MoO_3–Al_2O_3 catalyst. *J. Catal.* **61**, 115 (1980).
41. I.A. Van Parijs, L.H. Hosten, and G.F. Froment: Kinetics of the hydrodesulfurization on a cobalt–molybdenum/.gamma.–alumina catalyst. 2. Kinetics of the hydrogenolysis of benzothiophene. *Ind. Eng. Chem. Prod. Res. Dev.* **25**, 437 (1986).
42. T.C. Ho and J.E. Sobel: Kinetics of dibenzothiophene hydrodesulfurization. *J. Catal.* **128**, 581 (1991).
43. J.H. Kim, X. Ma, C. Song, Y-K. Lee, and S.T. Oyama: Kinetics of two pathways for 4,6-dimethyldibenzothiophene hydrodesulfurization over NiMo, CoMo sulfide, and nickel phosphide catalysts. *Energy Fuels* **19**, 353 (2005).
44. A. Tuxen, J. Kibsgaard, H. Gøbel, E. Lægsgaard, H. Topsøe, J.V. Lauritsen, and F. Besenbacher: Size threshold in the dibenzothiophene adsorption on MoS_2 nanoclusters. *ACS Nano* **4**, 4677 (2010).
45. A.K. Tuxen, H.G. Füchtbauer, B. Temel, B. Hinnemann, H. Topsøe, K.G. Knudsen, F. Besenbacher, and J.V. Lauritsen: Atomic-scale insight into adsorption of sterically hindered dibenzothiophenes on MoS_2 and Co–Mo–S hydrotreating catalysts. *J. Catal.* **295**, 146 (2012).
46. P. Zheng, A. Duan, K. Chi, L. Zhao, C. Zhang, C. Xu, Z. Zhao, W. Song, X. Wang, and J. Fan: Influence of sulfur vacancy on thiophene hydrodesulfurization mechanism at different MoS_2 edges: A DFT study. *Chem. Eng. Sci.* **164**, 292 (2017).
47. S. Helveg, J.V. Lauritsen, E. Lægsgaard, I. Stensgaard, J.K. Nørskov, B.S. Clausen, H. Topsøe, and F. Besenbacher: Atomic-scale structure of single-layer MoS_2 nanoclusters. *Phys. Rev. Lett.* **84**, 951 (2000).
48. A.M. Silva and I. Borges: How to find an optimum cluster size through topological site properties: MoS_x model clusters. *J. Comput. Chem.* **32**, 2186 (2011).
49. Y-W. Li, X-Y. Pang, and B. Delmon: Ab initio study of the structural and electronic properties of a real size MoS_2 slab: $Mo_{27}S_{54}$. *J. Phys. Chem. A* **104**, 11375 (2000).
50. H. Orita, K. Uchida, and N. Itoh: Ab initio density functional study of the structural and electronic properties of an MoS_2 catalyst model: A real size $Mo_{27}S_{54}$ cluster. *J. Mol. Catal. A: Chem.* **195**, 173 (2003).
51. X-D. Wen, T. Zeng, Y-W. Li, J. Wang, and H. Jiao: Surface structure and stability of MoS_x model clusters. *J. Phys. Chem. B* **109**, 18491 (2005).
52. B. Delley: An all-electron numerical method for solving the local density functional for polyatomic molecules. *J. Chem. Phys.* **92**, 508 (1990).
53. B. Delley: Fast calculation of electrostatics in crystals and large molecules. *J. Phys. Chem.* **100**, 6107 (1996).
54. B. Delley: From molecules to solids with the $DMol_3$ approach. *J. Chem. Phys.* **113**, 7756 (2000).
55. A. Bergner, M. Dolg, W. Küchle, H. Stoll, and H. Preuß: Ab initio energy-adjusted pseudopotentials for elements of groups 13–17. *Mol. Phys.* **80**, 1431 (1993).
56. D. Andrae, U. Häußermann, M. Dolg, H. Stoll, and H. Preuß: Energy-adjusted ab initio pseudopotentials for the second and third row transition elements. *Theor. Chim. Acta* **77**, 123 (1990).
57. Y. Inada and H. Orita: Efficiency of numerical basis sets for predicting the binding energies of hydrogen bonded complexes: Evidence of small basis set superposition error compared to Gaussian basis sets. *J. Comput. Chem.* **29**, 225 (2008).
58. J.P. Perdew and Y. Wang: Accurate and simple analytic representation of the electron-gas correlation energy. *Phys. Rev. B* **45**, 13244 (1992).
59. X-D. Wen, T. Zeng, B-T. Teng, F-Q. Zhang, Y-W. Li, J. Wang, and H. Jiao: Hydrogen adsorption on a $Mo_{27}S_{54}$ cluster: A density functional theory study. *J. Mol. Catal. A: Chem.* **249**, 191 (2006).
60. B. Delmon: Advances in hydropurification catalysts and catalysis. In *Studies in Surface Science and Catalysis*, D.L. Trimm, S. Akashah, M. Absi-Halabi, and A. Bishara, eds. (Elsevier, Amsterdam, the Netherlands, 1989); p. 1.
61. S.Y. Li, J.A. Rodriguez, J. Hrbek, H.H. Huang, and G.Q. Xu: Reaction of hydrogen with SMo(110) and MoS_x films: Formation of hydrogen sulfide. *Surf. Sci.* **366**, 29 (1996).
62. X. Liu, A. Tkalych, B. Zhou, A.M. Köster, and D.R. Salahub: Adsorption of hexacyclic C_6H_6, C_6H_8, C_6H_{10}, and C_6H_{12} on a Mo-terminated α-Mo_2C (0001) surface. *J. Phys. Chem. C* **117**, 7069 (2013).
63. M. Houalla, D.H. Broderick, A.V. Sapre, N.K. Nag, V.H.J. de Beer, B.C. Gates, and H. Kwart: Hydrodesulfurization of methyl-substituted dibenzothiophenes catalyzed by sulfided Co–Mo-γ-Al_2O_3. *J. Catal.* **61**, 523 (1980).
64. F. Bataille, J-L. Lemberton, P. Michaud, G. Pérot, M. Vrinat, M. Lemaire, E. Schulz, M. Breysse, and S. Kasztelan: Alkyldibenzothiophenes hydrodesulfurization-promoter effect, reactivity, and reaction mechanism. *J. Catal.* **191**, 409 (2000).
65. V. Meille, E. Schulz, M. Lemaire, and M. Vrinat: Hydrodesulfurization of alkyldibenzothiophenes over a NiMo/Al_2O_3 catalyst: Kinetics and mechanism. *J. Catal.* **170**, 29 (1997).
66. P. Michaud, J.L. Lemberton, and G. Pérot: Hydrodesulfurization of dibenzothiophene and 4,6-dimethyldibenzothiophene: Effect of an acid component on the activity of a sulfided NiMo on alumina catalyst. *Appl. Catal., A* **169**, 343 (1998).
67. R. Romero-Rivera, A.G. Camacho, M. Del Valle, G. Alonso, S. Fuentes, and J. Cruz-Reyes: HDS of DBT with molybdenum disulfide catalysts prepared by in situ decomposition of alkyltrimethylammonium thiomolybdates. *Top. Catal.* **54**, 561 (2011).
68. W. Trakarnpruk and B. Seentrakoon: Hydrodesulfurization activity of MoS_2 and bimetallic catalysts prepared by in situ decomposition of thiosalt. *Ind. Eng. Chem. Res.* **46**, 1874 (2007).
69. P.G. Moses, B. Hinnemann, H. Topsøe, and J.K. Nørskov: The hydrogenation and direct desulfurization reaction pathway in thiophene hydrodesulfurization over MoS_2 catalysts at realistic conditions: A density functional study. *J. Catal.* **248**, 188 (2007).

Supplementary Material

To view supplementary material for this article, please visit https://doi.org/10.1557/jmr.2018.309.